EXPERIMENTAL RESULTS ON SEDIMENT ENTRAINMENT BY GRAVITY CURRENTS

JESSICA ZORDAN[(1)], CARMELO JUEZ[(2)], ANTON J. SCHLEISS[(3)] & MÁRIO J. FRANCA[(4)]

[(1,2,3,4)] Laboratoire de Constructions Hydrauliques, École Polytechnique Fédérale de Lausanne, Switzerland
jessica.zordan@epfl.ch

ABSTRACT

Gravity currents are geophysical flows responsible of the distal transport of high volumes of sediments. In particular, turbidity currents, a form of gravity currents where sediments in suspension confer the buoyancy that ignites the flow, are the main mechanism for distal sediment transport within lakes and reservoirs. In maritime environment, submarine clay-rich gravity currents can impact and may endanger human made infrastructures such as submarine cables and platforms. It is thus important to understand the dynamics of sediment transport associated to gravity currents. In the present research, it is intended to experimentally investigate the mechanisms of entrainment, transport and deposition of fine sediments caused by the passage of a saline gravity current. Conservative saline currents, with varied initial density, are let to flow over an erodible bed sector where fine sediments, with three different grain sizes, are at rest. A detailed description of the gravity current dynamics is reported using 3D instantaneous velocities measurements over a certain profile. Video records obtained synoptically and laterally through a transparent wall, provide a visualization of the entrainment and resuspension processes which is further related to the flow hydrodynamics. The critical threshold conditions for initiating sediment motion is frequently related to the balance of boundary shear stress and the submerged weight of the particle. However boundary shear stress is just one of several impelling forces and the particle submerged weight is just one of several inertial forces. Here the attention is first focused on the complete description of the flow velocity, in term of instantaneous and mean flow. A deep analysis of the hydrodynamic of one gravity current reproduced in laboratory is here presented and its role in sediments' entrainment discussed.

Keywords: Gravity currents; sediment entrainment; erodible bed; 3D instantaneous velocities profiles.

1 INTRODUCTION

In atmosphere and in water, examples of gravity currents are numerous. In most of the examples that we can find in nature this buoyancy driven flows interact with sediments. Considering the cases of lava flows, dust storms or snow avalanches: the presence of sediments increases the density of the fluid which getting in contact with the lighter ambient air forms gravity currents. In water, suspended sediments at relative high concentration cause the formation of turbidity currents. A common point for these flows is their high interaction with the material of the bed surface. Travelling on a surface that is generally composed of erodible sediments, entrainment and eventually deposition of material can take place at a rate that depends on the characteristics of both the current and of the bed. Furthermore, gravity currents in nature occurs over complex topographies and varied bed compositions.

In situ measurements of gravity current have been documented (Xu et al., 2004; Paull et al., 2002) among others) and in many cases such flows are major and often catastrophic agents of sediment transport, both on land and within the ocean (Kneller et al. 2000). Gravity currents have been widely studied through both numerical (Ooi et al., 2009; Adduce et al., 2011; Ottolenghi et al., 2013; Lombardi et al., 2015) and experimental (Britter and Linden, 1980; Huppert and Simpson, 1980; Altinakar et al., 1990; Garcia and Parker, 1993; Shin et al., 2004; Nogueira et al., 2013a; Nogueira et al., 2013b; Theiler and Franca, 2016) simulations. Despite the wide interest on the topic, the mechanisms behind the interaction between the highly turbulent gravity current and the bed over which it flows, at the bottom interface, are not yet completely understood. Few contributions focus on a detail description of current hydrodynamic at the lower boundary and even less on the ability of a gravity current to entrain material from the bed. In the present study, in order to analyze the contribution of sediments coming from the mobile bed, saline conservative currents experiments have been carried over erodible bed. Three initial current densities have been tested combined with three different sediment grain sizes conforming the erodible bed.

The set-up was specifically design to perform full-depth lock-exchange experiments. The standard configuration, previously used by many authors (Huppert and Simpson, 1980; Rottman and Simpson, 1983; Adduce et al., 2011; Nogueira et al., 2014), was here adjusted in order to form an extended slumping phase in which the front velocity is almost constant (Tokyay et al., 2011). The initial volume of denser fluid is here comparable to the volume of the ambient water in the second part of the channel (Shin et al., 2004). The

bottom is horizontal and smooth. In these conditions, a quasi-steady regime is formed, similar to the steady state observed for constant feed gravity currents (Zordan et al., 2016).

This is particularly important since the dynamics of the near-bed region of such currents, which is characterized by high sediments concentration, is still poorly understood, as it is governed by intense particle-fluid and particle-particle interactions that give rise to mass and momentum exchanges between the current and the sediment bed. The coupling between the evolution of the gravity current and that of the underlying substrate is explored by analyzing the velocity profiles and the videos recorded from the side.

The present paper is structured as follows: first, the experimental set-up and the instrumentations are described. Subsequently, the results in term of streamwise and vertical velocity temporal evolutions and sediments entrainment from video analysis are presented. In the final section, the main findings are summarized and discussed looking at the possible further steps.

2 METHODS

2.1 Experimental set-up

The flume that was used to reproduce the gravity currents is 7.5 m long and 0.275 m wide and it is divided into two sections of comparable volumes by a vertically sliding gate (Figure 1). An upstream reach serves as head tank for the dense mixture (n.1 in Figure 1); a downstream reach is where the current propagates and where the main measurements are made. The bottom is horizontal and smooth along the whole channel apart for a section of 0.6 m of length, 2.5 m downstream the gate (n.2 in Figure 1). Here a mobile bed is localized and recreated by fulfilling a depression in the bed with sediments. The so called lock exchange technique is used: when the gate is removed, differences in the hydrostatic pressure cause the denser fluid to flow in one direction near the bottom boundary of the tank, while the lighter fluid flows in the opposite direction at the top (Shin et al., 2004). Downstream, the current is let to dissipate flowing down into a final large tank (n.3 in Figure 1).

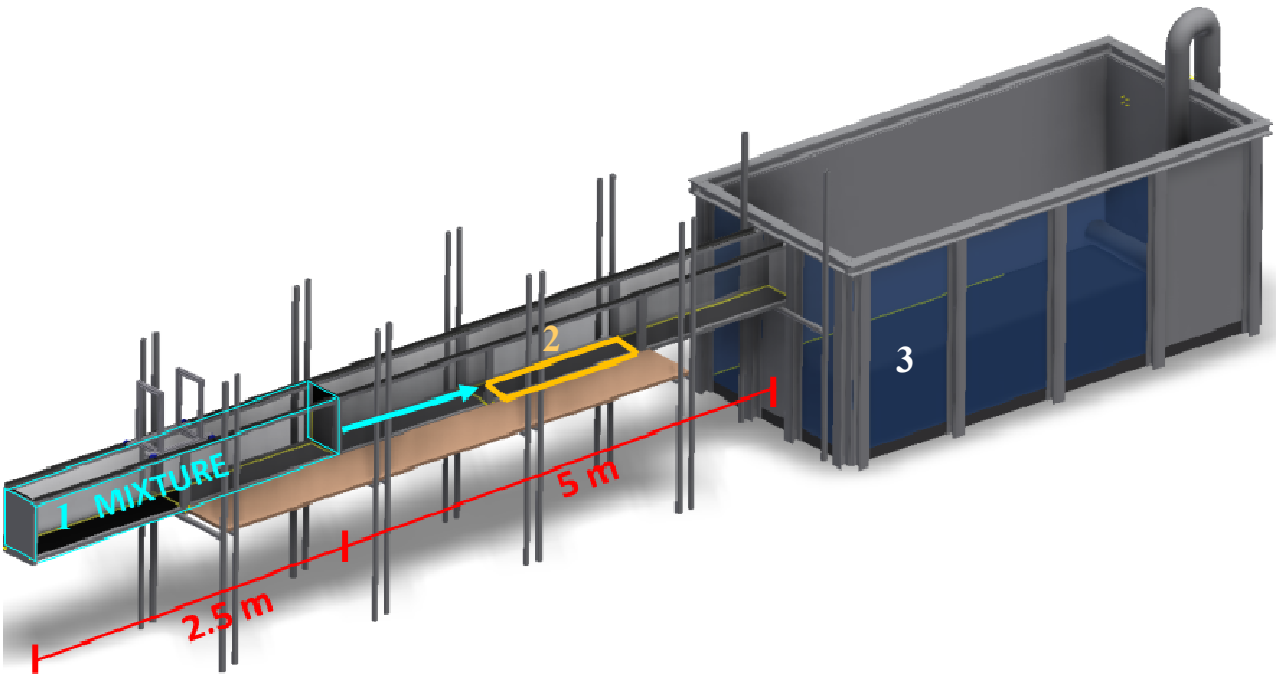

Figure 1. 3D view of the experimental set-up.

2.2 Measurements and instrumentation

The 3D Acoustic Doppler Velocity Profiler (ADVP) (Lemmin and Rolland, 1997, Franca and Lemmin, 2006) is a non-intrusive sonar instrument that measures the instantaneous velocity profiles using the Doppler effect without the need of calibration. It is placed right before the mobile bed and takes 3D instantaneous velocity measurements during the passage of the density current over a vertical, including the upper counter flow. For studies of turbulent flow, a high sampling frequency is desirable. The minimum number of pulse-pairs was here fixed at 32, in reason of our working conditions, which corresponds to a frequency of acquisition of 31.25 Hz (Lemmin and Rolland, 1997). The instrument consists of a central emitter surrounded by four receivers. The geometric configuration is the result of an optimization of the instrument that allows noise reduction by creating redundancy information for the velocity components (Blanckaert and Lemmin, 2006). This, together with the despiking procedure proposed by Goring and Nikora (2002), leads to a considerable

reduction in the noise level of the data set. The analysis of the power spectra of the raw data collected with the ADVP allows the identification of the noisy frequencies that where furthermore cut off through a low-pass filter of the signal.

The high-speed camera SMX-160 records the evolution of the gravity current over the erodible bed laterally, from the transparent side. The acquisition frequency was 25 Hz and the area of interest had a resolution of 500 x 180 pixels. The images are converted to grey-scale matrices for being post-processed. The interface between the water and the density current is identified by the subtraction between the current image and the initial image (without the current). The current passing over the mobile bed takes in suspension the material from the bottom. More challenging was the detection of the limit between current and sediment in suspension. A threshold for the identification of the pixels needed to be estimated. At the beginning of the experiments the pixel value associated to the sediments is annotated. Then, this value is used as reference threshold to identify pixels characterized by the presence of sediments, considering an average value of a group of neighboring pixels.

2.3 Experimental parameters

The experimental parameters of the nine tests performed are shown in Table 1 where ρ_0 is the gravity current initial density (as measured with a densimeter in the upstream reach), ρ_a is the ambient water density (998 kg/m^3), g is gravity and g' is the initial reduced gravity of the dense fluid defined as:

$$g' = g\frac{\rho_0 - \rho_a}{\rho_a} \quad [1]$$

Fr is the bulk densimetric Froude number derived for each test as:

$$Fr_D = \frac{u_f}{\sqrt{g'h_c}} \quad [2]$$

with h_c the average height of the current (one third of the total height of the fluid in the channel H=0.2m) and u_f the velocity of propagation of the front. Re_0, the Reynolds number based on the initial quantities, is determined as:

$$Re_0 = \frac{Uh_c}{\nu} \quad [3]$$

Where v is the kinematic viscosity and $U = \sqrt{g'h_c}$ the buoyancy velocity.

. **Table 1**. Experimental parameters for all experiments

Exp.	ρ_0 kg/m^3	g' m^2/s	u_f m/s	Re_0 x10^3	Fr_D -	D_{50} µm
R1.FINE	1028	0.29	0.101	48.2	0.593	80
R1.MEDIUM	1028	0.29	0.106	48.2	0.689	145
R1.COARSE	1028	0.29	0.126	48.2	0.771	91
R2.FINE	1038	0.39	0.117	55.7	0.595	80
R2.MEDIUM	1038	0.39	0.134	55.7	0.678	145
R2.COARSE	1038	0.39	0.127	55.7	0.646	191
R3.FINE	1048	0.49	0.131	62.4	0.595	80
R3.MEDIUM	1048	0.49	0.142	62.4	0.642	145
R3.COARSE	1048	0.49	0.155	62.4	0.704	191

The front velocity was computed through video analysis. The characteristic of the particle in terms of D_{50} (µm) is also given.

3 RESULTS

3.1 Flow velocity

The velocity data collected consists of instantaneous 3D velocity profiles along a vertical. Mean velocities where calculated by moving averaging the low-pass filtered instantaneous velocities following Baas et al. (2005). The time scale of the moving average was chosen by analyzing the power spectra of the

instantaneous low-passed signals. The maximum time window which allowed to still recognize the characteristic frequencies of the signal was taken in order to apply the moving averaging. One characteristic test will be here deeply analyzed. In Figure 2 the mean streamwise and vertical velocities fields, together with the vector field, for test R2.medium is reported. The vertical length scale was normalized by the total water height (H=0.2m). The regions of the current can be identified. The head height is larger than the body of the current and it presents a three-dimensional velocity structure. High streamwise velocities are presented within the head and Kelvin-Helmholtz billows are generated on the front of the head. This turbulent structures are generally associated with high mixing (Britter and Simpson, 1978). While the current advances, a return flow forms on the upper ambient fluid layer. This counter-current shows a jet-flow configuration as displayed by the mean streamwise velocity field (Figure 2, first plot).

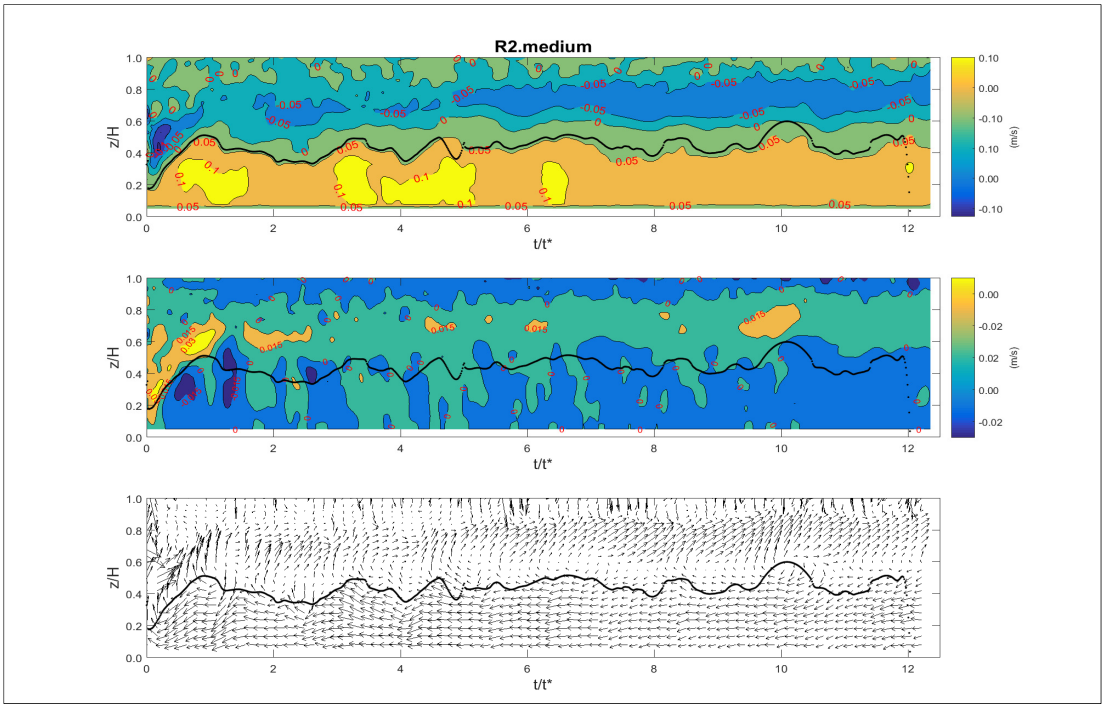

Figure 2. Mean streamwise (top) and vertical velocity field (middle) and vector field (bottom) for test R2.medium.

Peak of alternatively high positive and negative vertical velocities are present at the base of the current, near the bed. The advancing front causes a high-speed upward displacement of fluid that moves backward over the current's head.

The temporal evolution of the streamwise and vertical velocities are plotted for four different heights from the bed (Figure 3). The distances 18.8 mm, 31.3 mm, 52.1 mm and 72.9 mm have been considered as representative heights of the current. The highest streamwise velocities are detected at a distance of 18.8 mm from the bed. At 72.9 mm the streamwise velocities drop down and become negative: at this height the zone behind the head, characterized by a backward movement, is detected. The temporal evolution of the vertical velocities confirms the presence of upward and downward displacement of fluid, that are consistent along the whole vertical of the current. The highest values are recorded in the zone where the ambient water, pushed by the approaching front of the current, is displaced above and behind the head.

3.2 Sediments entrainment

Video analysis allows to track the sediments getting into suspension from the mobile bed. It was possible to compute the time evolution of the area occupied by the sediments by identifying the pixels occupied by the sediments in each picture taken. The same was done for the pixels belonging to the current. The areas of sediments and current are plotted in Figure 4 with the mean vertical velocities recorded at the closest recorded height from the bottom. It appears that the initiation of sediments entrainment begins in correspondence of the highest peak of vertical velocity. The time evolution of the current, as reported in Figure 4, shows that a peak is reached at around t/t^*=1, followed by a reduction. In fact the upper boundary of the current, at the interface with the ambient water, does not seem to be affected by the sediment's entrainment: the reduction of the height of the current, starting from around t/t^*=1, is rather related to the passage of the head which arises with respect to the body.

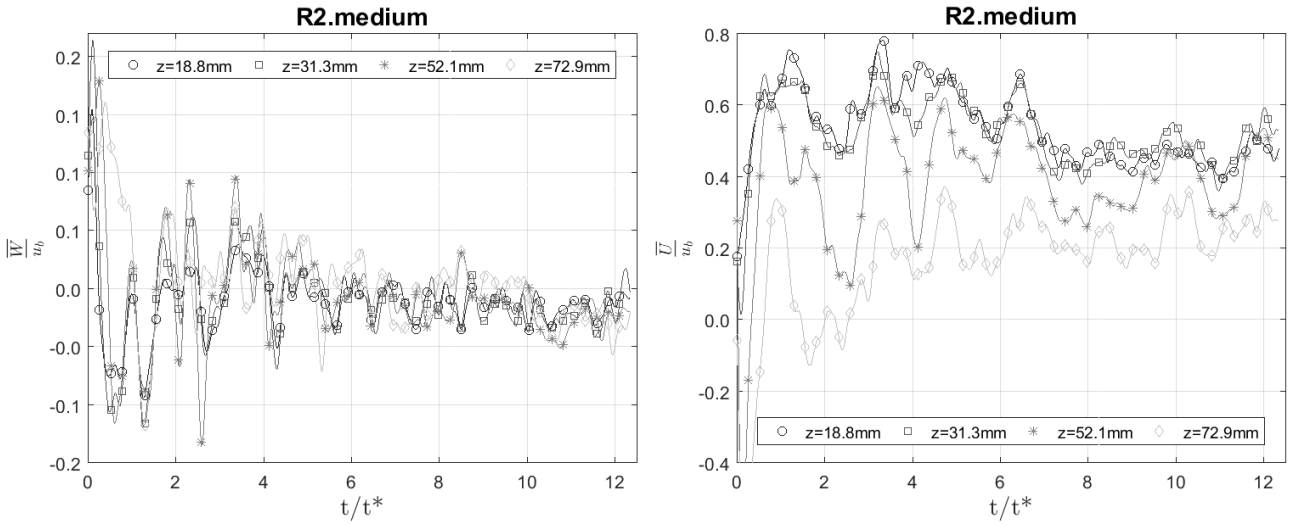

Figure 3. Streamwise (left) and vertical mean velocities (right) as a function of normalized time at four different elevations from the bed, for test *R2.medium*.

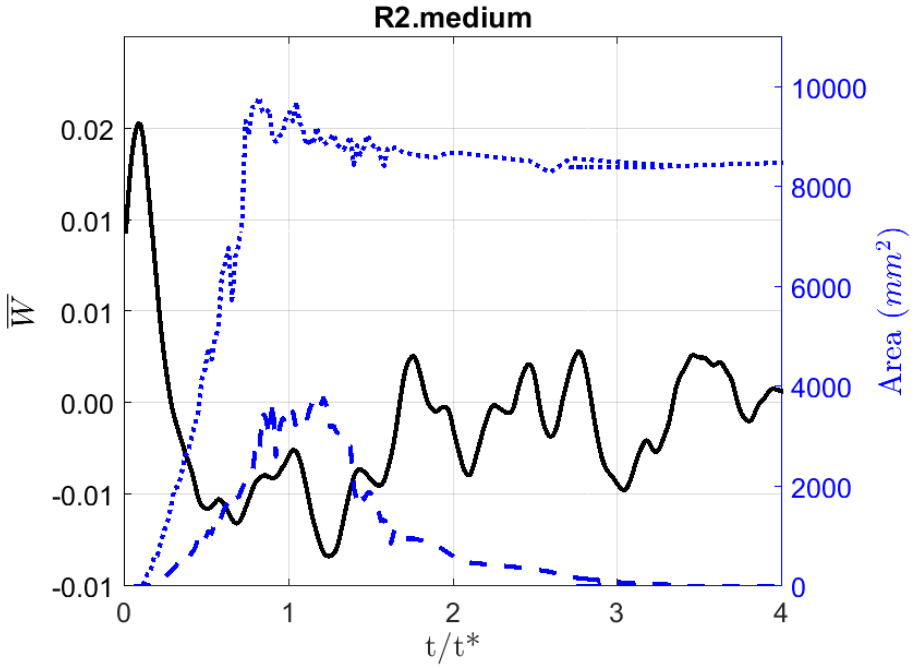

Figure 4. Time evolution of vertical velocity at the closest recorded height from the bottom (solid line), area of the current (dotted line) and of sediments (dashed line) from video processing.

4 CONCLUSION AND DISCUSSION

These preliminary results, allow to understand the mechanisms underlying the erosion and deposition processes. For this purpose, 3D-ADVP measurements have been performed, obtaining high resolution data for the velocities of the current before reaching the erodible bed. Velocity field provided useful information on the characteristics of the flow approaching the mobile bed. A peak in vertical upward velocity is present at the first instants of the front. The sediments entrainment was recorded with the high speed camera and the image processing allows to compute the time evolution of the area occupied by the sediments per each time frame. After synchronization of the measurements coming from the two instruments (ADVP and camera), the correspondence between mean vertical upward velocity and beginning of entrainment was highlighted. If the vertical velocity field can be related to the beginning of sediments motion, the author of sediments suspension subsistence needs to be identified. Moreover, a threshold at which the inertial forces overcome the impelling ones, implying sediments deposition, will be possibly determined. These are still open fields of study that will be addressed in the following of this research by investigating as well the role in the entrainment of sediments of bottom shear stress and of the turbulent quantities.

ACKNOWLEDGEMENTS

This research was funded by the European project SEDITRANS funded by Marie Curie Actions, FP7-PEOPLE-2013-ITN-607394 (Multi partner - Initial Training Networks).

REFERENCES

Adduce, C., Sciortino, G. & Proietti, S. (2011). Gravity Currents Produced by Lock Exchanges: Experiments and Simulations with a Two-Layer Shallow-Water Model with Entrainment. *Journal of Hydraulic Engineering*, 138(2), 111-121.

Altinakar, S., Graf, W.H. & Hopfinger, E.J. (1990). Weakly Depositing Turbidity Current on a Small Slope. *Journal of Hydraulic Research*, 28(1), 55-80.

Baas, J.H., McCaffrey, W.D., Haughton, P.D. & Choux, C. (2005). Coupling between Suspended Sediment Distribution and Turbulence Structure in a Laboratory Turbidity Current. *Journal of Geophysical Research: Oceans*, 110, 1-20.

Blanckaert, K. & Lemmin, U. (2006). Means of Noise Reduction in Acoustic Turbulence Measurements. *Journal of Hydraulic Research*, 44(1), 3–17.

Britter, R.E. & Simpson, J E. (1978). Experiments on the Dynamics of a Gravity Current Head. *Journal of Fluid Mechanics*, 88(02), 223-240.

Britter, R.E. & Linden, P. F. (1980). The Motion of the Front of a Gravity Current Travelling Down an Incline. *Journal of Fluid Mechanics*, 99(03), 531-543.

Garcia, M. & Parker, G. (1993). Experiments on the Entrainment of Sediment into Suspension by a Dense Bottom Current. *Journal of Geophysical Research*, 98, 4793-4793.

Goring, D.G. & Nikora, V.I. (2002). Despiking Acoustic Doppler Velocimeter Data. *Journal of Hydraulic Engineering*, 128(1), 117-126.

Franca, M.J. & Lemmin, U. (2006). Eliminating Velocity Aliasing in Acoustic Doppler Velocity Profiler Data. *Measurement Science and Technology*, 17(2), 313-322.

Huppert, H.E. & Simpson, J.E. (1980). The Slumping of Gravity Currents. *Journal of Fluid Mechanics*, 99(04), 785-799.

Kneller, B. & Buckee, C. (2000). The Structure and Fluid Mechanics of Turbidity Currents: A Review of Some Recent Studies and Their Geological Implications. *Sedimentology*, 47(1), 62-94.

Lemmin, U. & Rolland, T. (1997). Acoustic Velocity Profiler for Laboratory and Field Studies. *Journal of Hydraulic Engineering*, 12, 1089-1098.

Lombardi, V., Adduce, C., Sciortino, G. & La Rocca, M. (2015). Gravity Currents Flowing Upslope: Laboratory Experiments and Shallow-Water Simulations. *Physics of Fluids*, 27(1), 016602.

Nogueira, H.I., Adduce, C., Alves, E. & Franca, M.J. (2013). Analysis of Lock-Exchange Gravity Currents Over Smooth and Rough Beds. *Journal of Hydraulic Research*, 51(4), 417-431.

Nogueira, H.I., Adduce, C., Alves, E. & Franca, M.J. (2014). Dynamics of the Head of Gravity Currents. *Environmental Fluid Mechanics*, 14(2), 519-540.

Nogueira, H.I.S., Adduce, C., Alves, E. & Franca, M.J. (2014). Dynamics of the Head of Gravity Currents. *Environmental Fluid Mechanics*, 14(2), 519-540.

Ooi, S.K., Constantinescu, G. & Weber, L. (2009). Numerical Simulations of Lock-Exchange Compositional Gravity Current. *Journal of Fluid Mechanics*, 635, 361-388.

Ottolenghi, L., Adduce, C., Armenio, V., Inghilesi, R. & Roman, F. (2013). Gravity Currents Moving on Up-Sloping Boundaries. *Journal of Hydraulic Engineering,* 139(6), 593-601

Paull, C.K., Ussler, W., Greene, H.G., Keaten, R., Mitts, P. & Barry, J. (2002). Caught in the Act: The 20 December 2001 Gravity Flow Event in Monterey Canyon. *Geo-Marine Letters*, 22(4), 227-232.

Rottman, J.W. & Simpson, J.E. (1983). Gravity Currents Produced By Instantaneous Releases of a Heavy Fluid in a Rectangular Channel. *Journal of Fluid Mechanics*, 135, 95-110.

Shin, J.O., Dalziel, S.B. & Linden, P.F. (2004). Gravity Currents Produced By Lock Exchange. *Journal of Fluid Mechanics*, 521, 1-34.

Theiler, Q. & Franca, M.J. (2016). Contained Density Currents With High Volume Of Release. *Sedimentology*, 63(6), 1820-1842.

Tokyay, T., Constantinescu, G. & Meiburg, E. (2011). Lock-Exchange Gravity Currents with a High Volume of Release Propagating Over a Periodic Array of Obstacles. *Journal of Fluid Mechanics*, 672, 570-605.

Xu, J.P., Noble, M.A. & Rosenfeld, L.K. (2004). In-Situ Measurements of Velocity Structure within Turbidity Currents. *Geophysical Research Letters*, 31(9), 1-4.

Zordan, J., Schleiss, A.J. & Franca, M.J. (2016). *Bed Shear Stress Estimation for Gravity Currents Performed in Laboratory*, *River Flow 2016*. Taylor & Francis Group, London, 855-861 pp.

